

Post-LHC7 fine-tuning in the mSUGRA/CMSSM model with a 125 GeV Higgs boson

Howard Baer^a, Vernon Barger^b, Peisi Huang^b, Dan Mickelson^a, Azar Mustafayev^c and Xerxes Tata^c

^a*Dept. of Physics and Astronomy, University of Oklahoma, Norman, OK 73019, USA*

^b*Dept. of Physics, University of Wisconsin, Madison, WI 53706, USA*

^c*Dept. of Physics and Astronomy, University of Hawaii, Honolulu, HI 96822, USA*

E-mail: baer@nhn.ou.edu, barger@pheno.wisc.edu, phuang7@wisc.edu, dsmickelson@ou.edu, azar@phys.hawaii.edu, tata@phys.hawaii.edu

ABSTRACT: The recent discovery of a 125 GeV Higgs-like resonance at LHC, coupled with the lack of evidence for weak scale supersymmetry (SUSY), have severely constrained SUSY models such as mSUGRA/CMSSM. As LHC probes deeper into SUSY model parameter space, the little hierarchy problem – how to reconcile the Z and Higgs boson mass scale with the scale of SUSY breaking – will become increasingly exacerbated unless a sparticle signal is found. We evaluate two different measures of fine-tuning in the mSUGRA/CMSSM model. The more stringent of these, Δ_{HS} , includes effects that arise from the high scale origin of the mSUGRA parameters while the second measure, Δ_{EW} , is determined only by weak scale parameters: hence, it is universal to any model with the same particle spectrum and couplings. Our results incorporate the latest constraints from LHC7 sparticle searches, LHCb limits from $B_s \rightarrow \mu^+ \mu^-$ and also require a light Higgs scalar with $m_h \sim 123 - 127$ GeV. We present fine-tuning contours in the m_0 vs. $m_{1/2}$ plane for several sets of A_0 and $\tan \beta$ values. We also present results for Δ_{HS} and Δ_{EW} from a scan over the entire viable model parameter space. We find a $\Delta_{\text{HS}} \gtrsim 10^3$, or at best 0.1% fine-tuning. For the less stringent electroweak fine tuning, we find $\Delta_{\text{EW}} \gtrsim 10^2$, or at best 1% fine-tuning. Two benchmark points are presented that have the lowest values of Δ_{HS} and Δ_{EW} . Our results provide a quantitative measure for ascertaining whether or not the remaining mSUGRA/CMSSM model parameter space is excessively fine-tuned, and so could provide impetus for considering alternative SUSY models.

KEYWORDS: Fine-tuning, Supersymmetry Phenomenology, Supersymmetric Standard Model.

1. Introduction

The recent spectacular runs of LHC at $\sqrt{s} = 7$ and 8 TeV have led to identification of a Higgs-like boson¹ with mass $m_h \sim 125$ GeV [1, 2]. This is in accord with predictions from the minimal supersymmetric standard model (MSSM) which requires that the lighter higgs scalar mass $m_h \lesssim 130 - 135$ GeV [3]. Since values of $m_h > M_Z$ are only possible due to radiative corrections, the upper end of the range depends on the masses of third generation particles that one is willing to allow. To achieve $m_h \sim 125$ GeV, either large mixing or several TeV masses are required in the top squark sector. In models such as the much-studied minimal supergravity (mSUGRA or CMSSM) model [4, 5], values of trilinear soft breaking parameter $|A_0| \sim (1.5 - 2)m_0$ are favored, along with top squark masses $m_{\tilde{t}_{1,2}} \gtrsim 1 - 2$ TeV: for positive A_0 values m_0 is typically larger than 5 TeV [6, 7].

While the measured value of m_h is within the expected range of even the simplest SUSY models, there is at present no sign of SUSY particles at LHC. From LHC data analyses within the mSUGRA model, mass limits of $m_{\tilde{g}} \gtrsim 1.4$ TeV when $m_{\tilde{q}} \sim m_{\tilde{g}}$ and $m_{\tilde{g}} \gtrsim 0.9$ TeV when $m_{\tilde{q}} \gg m_{\tilde{g}}$ have been reported [8, 9]. Several groups [10] have updated their fits of the mSUGRA/CMSSM model to various data sets, now including information from LHC7 and LHC8 Higgs-like boson discovery and LHC7 sparticle mass limits. Typically, the best fit regions have moved out to large values of m_0 and $m_{1/2}$ to accomodate the LHC sparticle mass limits and Higgs discovery. Such large m_0 and $m_{1/2}$ values lead to sparticle masses in the multi-TeV mass range, thus exacerbating what has become known as *the little hierarchy problem*: how do such large SUSY particle masses and soft breaking parameters conspire to yield the weak scale typified by the Z -boson mass $M_Z \simeq 91.2$ GeV. The conflict between the strong new LHC sparticle mass limits and the comparatively low values of M_Z and m_h has intensified interest in the fine-tuning in supersymmetric models [11, 12, 13, 14, 15].

To set the stage for this analysis, we begin by reviewing radiative corrections (assumed perturbative) to scalar field masses. In a *generic* quantum field theory, taken to be the low energy effective theory whose domain of validity extends up to the energy scale Λ , the physical mass squared of scalar fields takes the schematic form (at leading order),

$$m_\phi^2 = m_{\phi 0}^2 + C_1 \frac{g^2}{16\pi^2} \Lambda^2 + C_2 \frac{g^2}{16\pi^2} m_{\text{low}}^2 \log \left(\frac{\Lambda^2}{m_{\text{low}}^2} \right) + C_3 \frac{g^2}{16\pi^2} m_{\text{low}}^2. \quad (1.1)$$

In Eq. (1.1), g denotes the typical coupling of the scalar ϕ , $m_{\phi 0}$ is the corresponding mass parameter in the Lagrangian, $16\pi^2$ is a loop factor, and C_i are constants that aside from spin, colour and other multiplicity factors are numbers $\mathcal{O}(1)$. The scales m_{low} and Λ respectively denote the highest mass scale in the effective theory and the scale at which this effective theory description becomes invalid because heavy degrees of freedom not included in the low energy Lagrangian become important. For instance, if we are considering corrections to the Higgs sector of the MSSM is embedded into a Grand Unified Theory (GUT) framework, $\Lambda \sim M_{\text{GUT}}$ and $m_{\text{low}} \sim M_{\text{SUSY}}$ (or more precisely, m_{low} is around the mass of

¹This particle has spin 0 or ≥ 2 and couples directly to the ZZ , and with weaker evidence also to the WW , systems. The latter property implies a connection with electroweak symmetry breaking, characteristic of the Higgs boson.

the heaviest sparticles that have large couplings to the scalar ϕ). Finally, the last term in (1.1) comes from loops of particles of the low energy theory, and their scale is set by m_{low} . These terms may contain logarithms, but *no large logarithms* since effects of very high momentum loops are included in the C_1 and C_2 terms. These finite corrections provide contributions to that which we have referred to as electroweak fine-tuning in a previous study[14].

If the effective theory description is assumed to be valid to the GUT scale, the C_1 term is enormous. Even so it is always possible to adjust the Lagrangian parameter $m_{\phi 0}^2$ to get the desired value of $m_{\phi^2} \lesssim m_{\text{low}}^2$. This is the *big fine tuning problem* of generic quantum field theory with elementary scalars. This problem is absent in softly broken supersymmetric theories because $C_1 = 0$. We see from Eq. (1.1) that if the physical value of m_ϕ is significantly smaller than m_{low} (which in the case of the MSSM $\sim m_{\tilde{t}_i}$), we will still need to have significant cancellations among the various terms to get the desired value of m_ϕ . This is the *little hierarchy problem*. We also see that in models such as mSUGRA that are assumed to be valid up to very high energy scales $\Lambda \sim M_{\text{GUT}} - M_P$, the magnitude of the C_2 term typically far exceeds that of the C_3 term because the logarithm is large, and hence is potentially the largest source of fine-tuning in such SUSY scenarios.

Because the C_2 and C_3 terms in Eq. (1.1) have somewhat different origins – the C_2 term represents corrections from physics at scales between m_{low} and Λ , while the C_3 term captures the corrections from physics at or below the scale m_{low} – we will keep individual track of these terms. In the following we will refer to fine-tuning from C_2 type terms as high scale fine-tuning (HSFT) (since this exists only in models that are valid to energy scales much larger than m_{low}) and to the fine tuning from C_3 -type terms as electroweak fine-tuning (EWFT) for reasons that are evident. We emphasize that the sharp distinction between these terms exists only in models such as mSUGRA that are assumed to be a valid description to very high scales, and is absent in low scale models such as the phenomenological MSSM [16].

In this paper, we quantify the severity of fine-tuning in the mSUGRA model, keeping separate the contributions from the two different terms. We are motivated to do so for two different reasons.

- First, as emphasized, C_2 type terms appear only if the theory is applicable out to scale $\Lambda \gg m_{\text{low}}$, while the C_3 type terms are always present. In this sense, the fine-tuning from the C_3 type terms is ubiquitous to all models, whereas the fine-tuning associated with the (potentially larger) C_2 type terms may be absent, depending on the model.
- Second, as we will explain below, there are two very different attitudes that one can adopt for the fine-tuning from C_2 type terms. Keeping the contributions from C_2 and C_3 separate will allow the reader the choice as to how to interpret our results and facilitate connection with previous studies.

The remainder of this paper is organized as follows. In Sec. 2 we introduce our measures of fine-tuning. As usual, we adopt the degree to which various contributions from the

minimization of the one-loop effective potential in the MSSM Higgs boson sector must cancel to reproduce the observed value of M_Z^2 as our measure of fine tuning. We use these considerations to introduce two different measures. The first of these is the less stringent one and relies only on the weak scale Lagrangian that arises from mSUGRA with total disregard for its high scale origin, and is referred to as electroweak fine-tuning (EWFT). The other measure that we introduce incorporates the high scale origin of mSUGRA parameters and is therefore referred to as high scale fine-tuning (HSFT). In Sec. 3, we present contours for both HSFT and EWFT in several mSUGRA m_0 *vs.* $m_{1/2}$ planes along with excluded regions from LHC7 sparticle searches and LHCb limits from $B_s \rightarrow \mu^+ \mu^-$ searches.² We find that while LHC7 sparticle mass limits typically require EWFT at $\sim 1\%$ level, the requirement that $m_h \sim 125$ GeV leads to much more severe EWFT in the 0.1% range in the bulk of parameter space. As anticipated, HSFT is even more severe. We also find that the hyperbolic branch/focus point region (HB/FP)[19] – while enjoying lower EWFT than the bulk of mSUGRA parameter space – still requires fine-tuning at about the percent level. The fine-tuning situation is exacerbated by the requirement of large $|A_0/m_0|$ for which the HB/FP region is absent, resulting in large EWFT (and even larger HSFT). In Sec. 4, we present results from a complete scan over mSUGRA/CMSSM parameter space. In this case, respecting both the LHC7 sparticle mass bounds, LHCb results on $B_s \rightarrow \mu^+ \mu^-$ and $m_h = 123 - 127$ GeV (in accord with the estimated theory error on our calculation of m_h), we find parameter space points with maximally 0.1% HSFT and 1% EWFT. We leave it to the reader to assess how much fine-tuning is too much, and also to judge the role of HSFT in models such as mSUGRA/CMSSM that originate in high scale physics. We present and qualitatively discuss the phenomenology of two model points with the lowest HSFT and the lowest EWFT in Sec. 5. We end with some concluding remarks and our perspective in Sec. 6.

2. Fine-tuning

We begin by first writing the Higgs potential whose minimization determines the electroweak gauge boson masses as,

$$V_{Higgs} = (m_{H_u}^2 + \mu^2)|h_u^0|^2 + (m_{H_d}^2 + \mu^2)|h_d^0|^2 - B\mu(h_u^0 h_d^0 + h.c.) + \frac{1}{8}(g^2 + g'^2)(|h_u^0|^2 - |h_d^0|^2)^2 + \Delta V, \quad (2.1)$$

where the radiative corrections (in the one-loop effective potential approximation) are given in the \overline{DR} scheme by,

$$\Delta V = \sum_i \frac{(-1)^{2s_i}}{64\pi^2} \text{Tr} \left((\mathcal{M}_i \mathcal{M}_i^\dagger)^2 \left[\log \frac{\mathcal{M}_i \mathcal{M}_i^\dagger}{Q^2} - \frac{3}{2} \right] \right). \quad (2.2)$$

²We note that Z-pole observables such as A_{FB}^b [17] and, according to recent calculation[18] also $R_b \equiv \frac{\Gamma(Z \rightarrow b\bar{b})}{\Gamma(Z \rightarrow \text{all})}$, appear to exhibit deviations at the $(2 - 2.5) \sigma$ level from Standard Model expectations. While these possible discrepancies merit a watchful eye, an attempt to account for them in a SUSY framework is beyond the scope of this paper.

Here, the sum over i runs over all fields that couple to Higgs fields, $\mathcal{M}_i \mathcal{M}_i^\dagger$ is the *Higgs field dependent* mass squared matrix (defined as the second derivative of the tree level potential), and the trace is over the internal as well as any spin indices. One may compute the gauge boson masses in terms of the Higgs field vacuum expectation values v_u and v_d by minimizing the scalar potential in the h_u^0 and h_d^0 directions. This leads to the well-known condition

$$\frac{M_Z^2}{2} = \frac{(m_{H_d}^2 + \Sigma_d^d) - (m_{H_u}^2 + \Sigma_u^u) \tan^2 \beta}{\tan^2 \beta - 1} - \mu^2. \quad (2.3)$$

Here the Σ_u^u and Σ_d^d terms arise from first derivatives of ΔV evaluated at the potential minimum and $\tan \beta \equiv v_u/v_d$. At the one-loop level, Σ_u^u contains the contributions $\Sigma_u^u(\tilde{t}_{1,2})$, $\Sigma_u^u(\tilde{b}_{1,2})$, $\Sigma_u^u(\tilde{\tau}_{1,2})$, $\Sigma_u^u(\tilde{W}_{1,2})$, $\Sigma_u^u(\tilde{Z}_{1-4})$, $\Sigma_u^u(h, H)$, $\Sigma_u^u(H^\pm)$, $\Sigma_u^u(W^\pm)$, $\Sigma_u^u(Z)$, and $\Sigma_u^u(t)$. Σ_d^d contains similar terms along with $\Sigma_d^d(b)$ and $\Sigma_d^d(\tau)$ while $\Sigma_d^d(t) = 0$ [14].

Although we have highlighted third generation matter sfermion contributions here because these frequently dominate on account of their large Yukawa couplings, we note that there are also first/second generation contributions $\Sigma_u^u(\tilde{q}, \tilde{\ell})$ and $\Sigma_d^d(\tilde{q}, \tilde{\ell})$ that arise from the quartic D -term interactions between the Higgs sector and matter scalar sector even when the corresponding Yukawa couplings are negligibly small. These contributions are proportional to $(T_{3_i} - Q_i \sin^2 \theta_W) \times F(m_i^2)$, where T_{3_i} is the hypercharge, Q_i is the electric charge and $F(m^2) = m^2(\log \frac{m^2}{Q^2} - 1)$ of the i^{th} matter scalar. Although the scale of these is set by the electroweak gauge couplings rather than the top Yukawa coupling, these can nevertheless be sizeable if the squarks of the first two generations are significantly heavier than third generation squarks. However, in models such as mSUGRA – where all squarks of the first two generations (and separately, the corresponding sleptons) are nearly mass degenerate – these contributions largely cancel. Indeed, the near cancellation (which would be perfect cancellation in the case of exact degeneracy) occurs within each generation, and separately for squarks and for sleptons. These terms, summed over each of the first two generations, are always smaller than the other terms in the C_i and B_i arrays used to define our fine-tuning criterion below, and so do not alter our fine-tuning measure defined below.

The reader may wonder that we are treating the first two generations differently from the third generation in that for the latter we consider the contributions from each squark separately (*i.e.* not allow for cancellations of the contributions to say Σ_u^u from different squarks to cancel), while we sum the contributions from the entire first/second generation to obtain a tiny contribution. The reason for this is that the mSUGRA framework *predicts* degenerate first/second generation squarks (and sleptons) while the top squark masses (remember that top squarks frequently make the largest contribution to Σ_u^u) are essentially independent. In an unconstrained framework such as the pMSSM [16] we *would not combine* the contributions from the first/second generation scalars; if these are very heavy and have large intra-generation splitting, their contribution to Δ_{EW} can be significant.

2.1 Electroweak scale fine-tuning

One measure of fine-tuning, introduced previously in Ref. [14, 12], is to posit that there are no large cancellations in Eq. (2.3). This implies that all terms on the right-hand side to be

comparable to $M_Z^2/2$, *i.e.* that each of the three tree level terms $C_{H_d} \equiv |m_{H_d}^2/(\tan^2 \beta - 1)|$, $C_{H_u} \equiv |-m_{H_u}^2 \tan^2 \beta/(\tan^2 \beta - 1)|$, $C_\mu \equiv |-\mu^2|$ and each $C_{\Sigma_{u,d}^i}$ is less than some characteristic value Λ where $\Lambda \sim M_Z^2$. (Here, i labels SM and supersymmetric particles that contribute to the one-loop Higgs potential and includes the sum over matter sfermions from the first two generations.) This leads to a fine-tuning measure

$$\Delta_{\text{EW}} \equiv \max(C_i)/(M_Z^2/2). \quad (2.4)$$

A feature of defining the fine-tuning parameter solely in terms of weak scale parameters is that it is independent of whether the SUSY particle spectrum is generated using some high scale theory or generated at or near the weak scale, as in the pMSSM or possibly in gauge-mediation [20]: if the spectra and weak scale couplings from two different high scale theories are identical, the corresponding fine-tuning measures are the same. However, as we will see in Subsection 2.2, in theories such as mSUGRA Δ_{EW} does not capture the entire fine-tuning because Eq. (2.3) does not include information about the underlying origin of the weak scale mass parameters.

It is worthwhile to note that over most of parameter space the dominant contribution to Δ_{EW} comes from the weak scale values of $m_{H_u}^2$ and μ^2 . To see this, we note that unless $\tan \beta$ is very small, aside from radiative corrections, we would have simply that $M_Z^2/2 \simeq -m_{H_u}^2 - \mu^2$. As is customary, the value of μ^2 is selected so that the correct value of M_Z is generated. In this case, over much of parameter space $\Delta_{\text{EW}} \sim |\mu^2|/(M_Z^2/2)$. Only when $|\mu|$ becomes small do the radiative corrections become important – providing the largest contribution to Eq. (2.3). Thus, contours of fixed Δ_{EW} typically track the contours of $|\mu|$ except when $|\mu|$ is small; in this latter case, Δ_{EW} is determined by the $|\Sigma_u^u|$ whose value is loop-suppressed. In Fig. 1 we show the surface of $|\mu|$ values in the m_0 *vs.* $m_{1/2}$ plane of mSUGRA/CMSSM for $A_0 = 0$ and $\tan \beta = 10$. Here, μ is small either at low m_0 and $m_{1/2}$ (the bulk region[21]), or in the HB/FP region[19] at large values of m_0 .

2.2 High scale fine-tuning

As mentioned above, Eq. (2.3) is obtained from the weak scale MSSM potential and so contains no information about its possible high scale origin. To access this, and make explicit the dependence on the high scale Λ , we must write the *weak scale* parameters $m_{H_{u,d}}^2$ in Eq. (2.3) as

$$m_{H_{u,d}}^2 = m_{H_{u,d}}^2(\Lambda) + \delta m_{H_{u,d}}^2, \quad \mu^2 = \mu^2(\Lambda) + \delta \mu^2,$$

where $m_{H_{u,d}}^2(\Lambda)$ and $\mu^2(\Lambda)$ are the corresponding parameters renormalized at the high scale Λ . It is the $\delta m_{H_{u,d}}^2$ terms that contain the $\log \Lambda$ dependence shown in the C_2 type terms in Eq. (1.1). In this way, we get

$$\frac{M_Z^2}{2} = \frac{(m_{H_d}^2(\Lambda) + \delta m_{H_d}^2 + \Sigma_d^d) - (m_{H_u}^2(\Lambda) + \delta m_{H_u}^2 + \Sigma_u^u) \tan^2 \beta}{\tan^2 \beta - 1} - (\mu^2(\Lambda) + \delta \mu^2). \quad (2.5)$$

Following the same spirit that we had used in our earlier analyses [14], we can now define a fine-tuning measure that encodes the information about the high scale origin of the

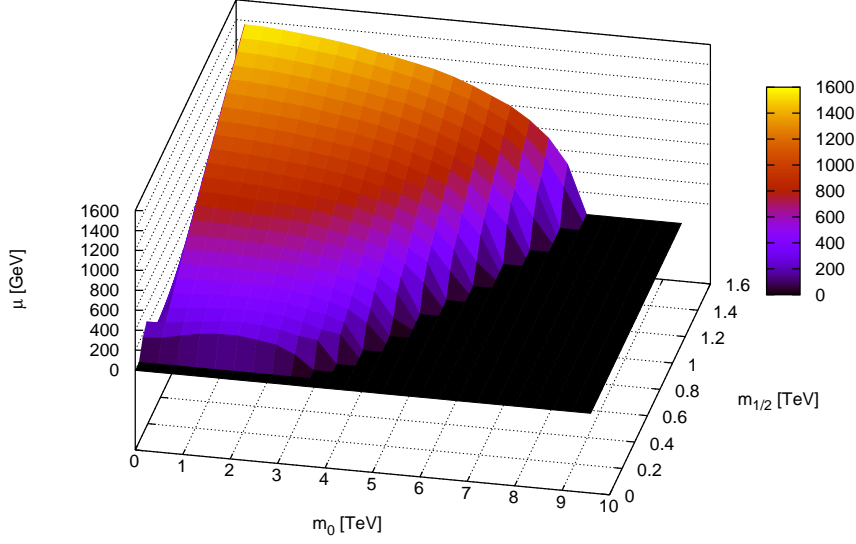


Figure 1: The value of μ in the m_0 vs. $m_{1/2}$ plane of mSUGRA for $A_0 = 0$ and $\tan\beta = 10$. We set $\mu = 0$ in theoretically forbidden regions.

parameters by requiring that each of the terms on the right-hand-side of Eq. (2.5) to be smaller than a pre-assigned Δ_{HS} times $\frac{M_Z^2}{2}$. The high scale fine-tuning measure Δ_{HS} is thus defined to be

$$\Delta_{\text{HS}} \equiv \max(B_i)/(M_Z^2/2), \quad (2.6)$$

with

$$B_{H_d} \equiv |m_{H_d}^2(\Lambda)/(\tan^2\beta - 1)|, \quad B_{\delta H_d} \equiv |\delta m_{H_d}^2/(\tan^2\beta - 1)|, \\ B_{H_u} \equiv |-m_{H_u}^2(\Lambda)\tan^2\beta/(\tan^2\beta - 1)|, \quad B_{\delta H_u} \equiv |-\delta m_{H_u}^2\tan^2\beta/(\tan^2\beta - 1)|, \text{ etc.},$$

defined analogously to the set C_i in Sec. 2.1. As discussed above, in models such as mSUGRA whose domain of validity extends to very high scales, because of the large logarithms one would expect that (barring seemingly accidental cancellations) the $B_{\delta H_u}$ contributions to Δ_{HS} would be much larger than any contributions to Δ_{EW} because the $m_{H_u}^2$ evolves from m_0^2 to negative values.

As we have noted, Δ_{EW} indeed provides a measure of EWFT that is determined only by the particle spectrum: by construction, it has no information about any tuning that may be necessary in order to generate a given weak scale SUSY mass spectrum. Thus, while for a given SUSY spectrum Δ_{EW} includes information about the *minimal amount of fine-tuning* that is present in the model, Δ_{HS} better represents the fine-tuning that is present in high scale models.

The reader may have noticed that – unlike in our definition of Δ_{EW} in Eq. (2.4) where we have separated out the contributions from various sources and required each of these to not exceed some preassigned value – we have neglected to separate out the various

contributions to $\delta m_{H_{u,d}}^2$ that determine Δ_{HS} . We have done so mainly for convenience,³ but this will also help us to connect up with what has been done in the literature.

Before closing this section, we remark that our definition of Δ_{HS} differs in spirit from that used by some groups[15]. These authors write the $m_{H_u}^2$ as a quadratic function of the high scale parameters $\xi_i = \{m_0, m_{1/2}, A_0\}$ for mSUGRA, *i.e.*

$$m_{H_u}^2 = \sum a_{ij} \xi_i \xi_j, \quad (2.7)$$

and substitute this (along with the corresponding form for $m_{H_d}^2$) in Eq. (2.3) to examine the sensitivity of M_Z^2 to changes in the high scale parameters.⁴ In the resulting expression, the coefficient of m_0^2 in Eq. (2.7) is often very small because of cancellations with the large logarithms, suggesting that the region of mSUGRA with rather large m_0 (but small $m_{1/2}$ and A_0) is not fine-tuned: we feel that this is misleading and so have *separated* the contributions from the large logarithms in our definition of Δ_{HS} . Combining all m_0^2 contributions into a single term effectively combines $m_i^2(\Lambda) + \delta m_i^2$ into a single quantity which (aside from the one-loop terms Σ_u^u and Σ_d^d) evidently is *the weak scale value of m_i^2* in our definition of Δ_{HS} . Except for these one-loop correction terms, Δ_{HS} then reduces to Δ_{EW} !

In defining Δ_{HS} as above, we have taken the view that the high scale parameters as well as the scale at which we assume the effective theory to be valid are independent. *In the absence of an underlying theory of the origin of these parameters*, we regard cancellations between terms in Eq. (2.7) that occur for *ad hoc* relations⁵ between model parameters and lead one to conclude that M_Z is not fine-tuned as fortuitous, and do not incorporate it into our definition of high scale fine-tuning. We emphasize that we would view the fine-tuning question very differently if indeed the high scale parameters were all related from an underlying meta-theory.⁶ In that case, though, as we just mentioned, Δ_{EW} would be an adequate measure of fine tuning.

3. Results in m_0 vs. $m_{1/2}$ plane

We present our first results as contours of Δ_{HS} and Δ_{EW} in the m_0 vs. $m_{1/2}$ plane of the mSUGRA/CMSSM model. For all plots, we take $m_t = 173.2$ GeV and we generate SUSY

³Unlike for Δ_{EW} where we have separated the contributions by particles (and treated these as independent) for the electroweak scale theory, in a constrained high scale model, these would not be independent. Instead, we could separate out contributions that have independent origins in the high scale model. For instance, for the mSUGRA model we should separately require contributions from gauginos, scalars and A -parameters to $\delta m_{H_i}^2$ to be small. We have not done so here mainly for expediency. In this sense if accidental cancellations reduce Δ_{HS} to very small values, this should be interpreted with care.

⁴Typically these authors use $\Delta \equiv \frac{a_i}{M_Z^2} \frac{\partial M_Z^2}{\partial a_i}$ (where a_i labels the input parameters) as a measure of the sensitivity to parameters[11]. This prescription agrees with our Δ at tree level, but differs when loop corrections are included.

⁵It may be argued that such an analysis is helpful as a guide to model builders attempting to construct models of natural SUSY.

⁶This situation seems to occur in the so-called mixed-modulus-anomaly mediated SUSY breaking models for some ranges of the mixing parameter α as emphasized in Ref. [22].

particle mass spectra from Isasugra v7.83 [23]. In Fig. 2, we show contours of Δ_{HS} in frame *a*) and for Δ_{EW} in frame *b*). For both frames, we take $A_0 = 0$, $\tan\beta = 10$ and $\mu > 0$. The gray-shaded regions running from the extreme left of the plot, across the bottom and on to the right are excluded by either a $\tilde{\tau}_1$ as LSP (left-side), LEP1 constraints (bottom) or lack of appropriate EWSB (right-side). The region marked LEP2 is excluded by LEP2 chargino searches ($m_{\tilde{W}_1} > 103.5$ GeV) [24]. The region below the contour labeled LHC7 is excluded by lack of a SUSY signal from SUSY searches at LHC7 with 5 fb^{-1} of data [8, 9]. The dashed portion of the contour is our extrapolation of LHC7 results to higher values of m_0 than are shown by the Atlas/CMS collaborations. We also denote regions where the calculated [25] branching fraction $B_s \rightarrow \mu^+ \mu^-$ falls outside its newly measured range from LHCb observations [26], which now require

$$2 \times 10^{-9} < BF(B_s \rightarrow \mu^+ \mu^-) < 4.7 \times 10^{-9} \quad (95\% \text{ CL}). \quad (3.1)$$

However, for the low value of $\tan\beta$ in this figure (and also in subsequent figures with $\tan\beta = 10$) the LHCb does not lead to any constraint because the SUSY contribution, which grows rapidly with $\tan\beta$, is rather small. The green-shaded region is where the thermally-generated relic density of neutralinos (computed using IsaReD [27]) satisfies $\Omega_{\tilde{Z}_1}^{\text{th}} h^2 < 0.1194$, the 2σ upper limit on the density of cold dark matter obtained by the WMAP collaboration [28]. This region encompasses the stau-coannihilation strip [29] (extreme left), the bulk region [21] (bottom left corner) and the well-known focus point/hyperbolic branch region [19] of the model. The shaded region labeled a_μ is where the measured muon magnetic moment [30] satisfies $4.7 \times 10^{-10} \leq a_\mu \leq 52.7 \times 10^{-10}$, within 3σ of its theoretical value [31]. For $A_0 = 0$ adopted in this figure, $m_h < 123$ GeV over the entire parameter plane, so that mSUGRA is excluded for $A_0 \sim 0$ (as noted in Ref. [6]) unless one has very high values of m_0 and $m_{1/2}$ [32].

As might be anticipated, Δ_{HS} grows with increasing values of m_0 or $m_{1/2}$, so that we expect contours of fixed Δ_{HS} to be oval-shaped in the $m_0 - m_{1/2}$ plane. This is readily seen in frame *a*) of Fig. 2, except that because the oval is extremely elongated since the scales on the two axes are very different, we see only a small part of this contour (which appears as nearly vertical lines) for very large values of Δ_{HS} . We have checked that $\Delta_{\text{HS}} < 150$ is already excluded by LHC searches, so high scale fine-tuning of less than a percent is now mandatory for $A_0 = 0$. If we take the high scale origin of the mSUGRA model seriously, we see that without a theory that posits special relations between the parameters that could lead to automatic cancellation of the large logarithms that enter Δ_{HS} , we are forced to conclude that LHC data imply that the theory is fine-tuned to a fraction of a percent. For the portion of the plane compatible with LHC constraints on sparticles, the smallest values of Δ_{HS} occur where m_0 and $m_{1/2}$ are simultaneously small. As m_0 moves to the multi-TeV scale, Δ_{HS} exceeds 1000, and fine-tuning of more than part per mille is required.

In frame *b*) of the figure, we show contours of constant Δ_{EW} . Over most of the plane, these contours tend to track contours of constant μ^2 since $M_Z^2/2 \sim -m_{H_u}^2 - \mu^2$ so that when $|m_{H_u}^2| \gg M_Z^2/2$, then $-m_{H_u}^2 \sim \mu^2$. Thus, along the contours of Δ_{EW} , the value of $m_{H_u}^2$ is independent of m_0 at least until the contours turn around at large values of m_0 and $m_{1/2}$.

This is just the focus point behaviour discussed in the second paper of Ref. [19].⁷ The Δ_{EW} contours, for large values of m_0 bend over and track excluded region on the right where μ^2 becomes negative. This is the celebrated hyperbolic branch [19] of small $|\mu|$. The contours of Δ_{EW} then bend around for very large values of m_0 because Σ_u^u contributions, especially from \tilde{t}_2 loops — increase with m_0 — begin to exceed $-m_{H_u}^2 \simeq \mu^2$. Indeed, Fig. 2b) shows that there is a region close to (but somewhat removed from) the “no EWSB” region on the right where Δ_{EW} becomes anomalously small even for large values of m_0 and $m_{1/2}$. It is instructive to see that while this low EWFT region is close to the relic-density consistent region with small μ [19], it is still separated from it.⁸ While $\Delta_{EW} \sim 100$ is excluded at low m_0 , this 1% EWFT contour, even with the resolution of our scan, extends out to very large $m_0 \sim 6$ TeV values for $m_{1/2}$ as high as 1 TeV! While these plots show that relatively low EWFT (Δ_{EW} of a few tens) is still allowed by LHC7 constraints on sparticles, it is important to realize that *these planes are now excluded since they cannot accommodate $m_h \sim 125$ GeV*.

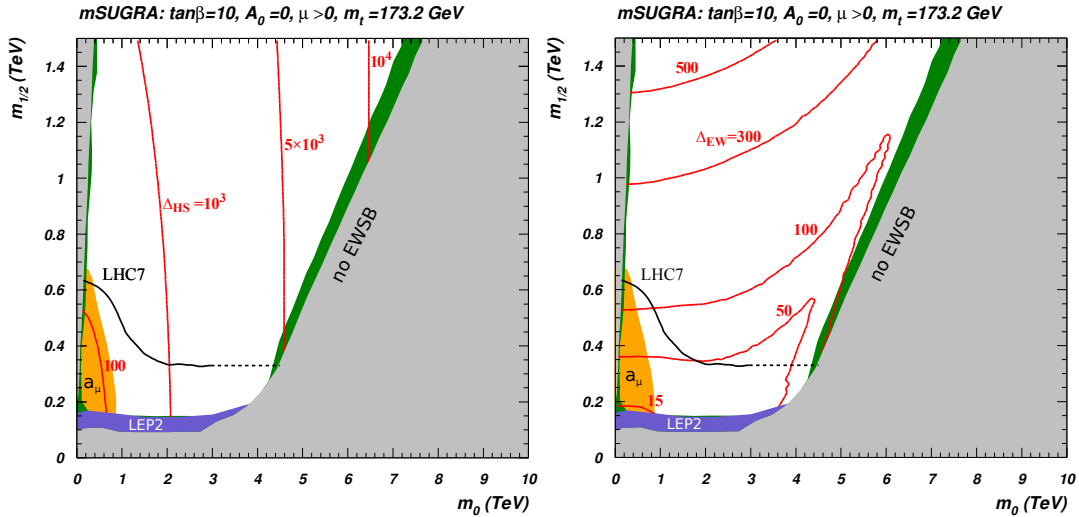


Figure 2: Contours of a) Δ_{HS} and b) Δ_{EW} in the mSUGRA model with $A_0 = 0$ and $\tan\beta = 10$. We take $\mu > 0$ and $m_t = 173.2$ GeV. The grey region on the left is excluded either because the stau is too light or becomes tachyonic, the grey region at the bottom is excluded by LEP1 constraints, while in the region on the right we do not get the correct pattern of EWSB, since either μ^2 or m_A^2 become negative. The region labeled LEP2 is excluded by constraints on the chargino mass. The region labeled a_μ is allowed at the 3σ level by the E821 experiment while in the green-shaded region, the thermal neutralino relic density is at or below the WMAP measurement of the cold dark matter density. The region below black contour labeled LHC7 is excluded by SUSY searches. The lighter Higgs boson mass $m_h < 123$ GeV throughout this parameter plane.

Before moving on to other planes, we remark that for the smallest values of m_0 in the

⁷More precisely, the discussion in this paper was for a fixed value of $m_{1/2}$ so that the range of m_0 was limited because we hit the theoretically excluded region. We see though that the same value of $m_{H_u}^2$ can be obtained if we simultaneously increase m_0 and $m_{1/2}$ so that we remain in the theoretically allowed region.

⁸Much of the literature treats these regions as one. While this is fine for some purposes, it seems necessary to be clear on the difference when discussing either dark matter or EWFT. Note that Δ_{HS} is large in both regions.

LHC-allowed regions of the figure, $\Delta_{\text{HS}} \sim \Delta_{\text{EW}}$. As we have explained, Δ_{HS} is determined by the value of $|\delta m_{H_u}^2|$ (see Eq. 2.5), which for $m_0 \sim 0$ is just $|m_{H_u}^2|$ that determined Δ_{EW} when m_0 is very small. We thus see that the two measures are roughly comparable for small values of m_0 but deviate from one another as m_0 is increased. We see that Δ_{HS} typically exceeds Δ_{EW} by an order of magnitude, because of the large logarithm of the ratio of the GUT and weak scales, except in the HB/FP region where Δ_{EW} is exceptionally small.

In Fig. 3 we show the m_0 vs. $m_{1/2}$ plane for $\tan\beta = 50$ and $A_0 = 0$. The contours in both frames are qualitatively very similar those for the $\tan\beta = 10$ case. As expected, regions of low Δ_{EW} extend to very large m_0 and $m_{1/2}$ in the HB region. One difference from the $\tan\beta = 10$ case discussed above is that this time the HB region largely overlaps with the relic-density-consistent green-shaded region. Note also that for this large value of $\tan\beta$ there is a considerable region (left of the LHCb contour) that is now excluded due to too large a value of $BF(B_s \rightarrow \mu^+\mu^-)$. Again, the entire region of plane shown is excluded by the LHC Higgs discovery at 125 GeV.

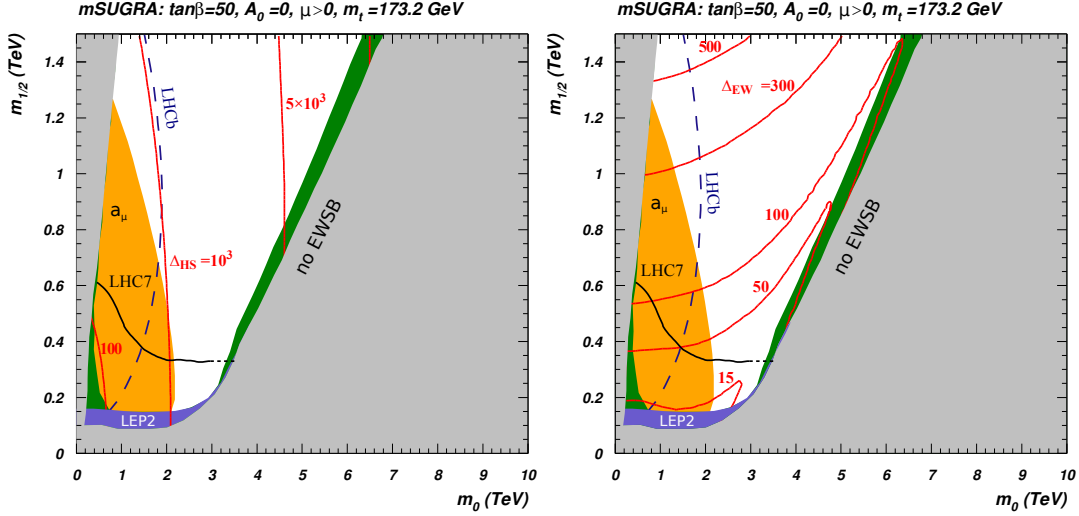


Figure 3: Contours of a) Δ_{HS} and b) Δ_{EW} in the mSUGRA model with $A_0 = 0$, $\tan\beta = 50$ and $\mu > 0$. The value of m_t as well as the various shaded/coloured regions are as in Fig. 2. The region to the left of the long dashed blue contour is excluded by LHCb measurements.

In Fig. 4, we show contours of Δ_{HS} and Δ_{EW} for $\tan\beta = 10$ and $A_0 = -m_0$. The first thing to notice is that the HB/FP region does not appear. The region at extremely large m_0 is still theoretically excluded, but more typically because m_A^2 turns negative (or there are tachyons) *not because* μ^2 *turns negative*.⁹ In addition, the very large $m_0 \gtrsim 7 - 9$ TeV region yields a value of $m_h > 123$ GeV: thus, the bulk of this plane is still excluded. The contours of Δ_{HS} are qualitatively similar to the $A_0 = 0$ cases, and LHC7 still excludes

⁹For $m_{1/2} = 500$ GeV, this happens for $m_0 \gtrsim 22$ TeV. We mention that this breakdown of parameter space could be an artifact of the ISAJET algorithm for computing the sparticle mass spectrum in mSUGRA. An approximate tree-level spectrum is first required in order to evaluate the radiative corrections that can potentially yield a valid solution using an iterative procedure. But in the absence of a non-tachyonic, tree-level spectrum with the correct EWSB pattern, the program is unable to compute the radiatively corrected mass spectrum.

$\Delta_{\text{HS}} < 100$, so again a HSFT of more than 1% is required. In the region with $m_h > 123$ GeV, $\Delta_{\text{HS}} \gtrsim 1.5 \times 10^4$, and extreme HSFT is required. Moving to frame b), we note that though the contours of fixed Δ_{EW} now run from top left to lower right, these still follow the lines of fixed values of μ^2 . Moreover, values of Δ_{EW} below 100 are excluded by just the LHC7 sparticle mass constraints. If one also imposes $m_h > 123$ GeV, then $\Delta_{\text{EW}} \gtrsim 2000$ is required over the entire plane shown.

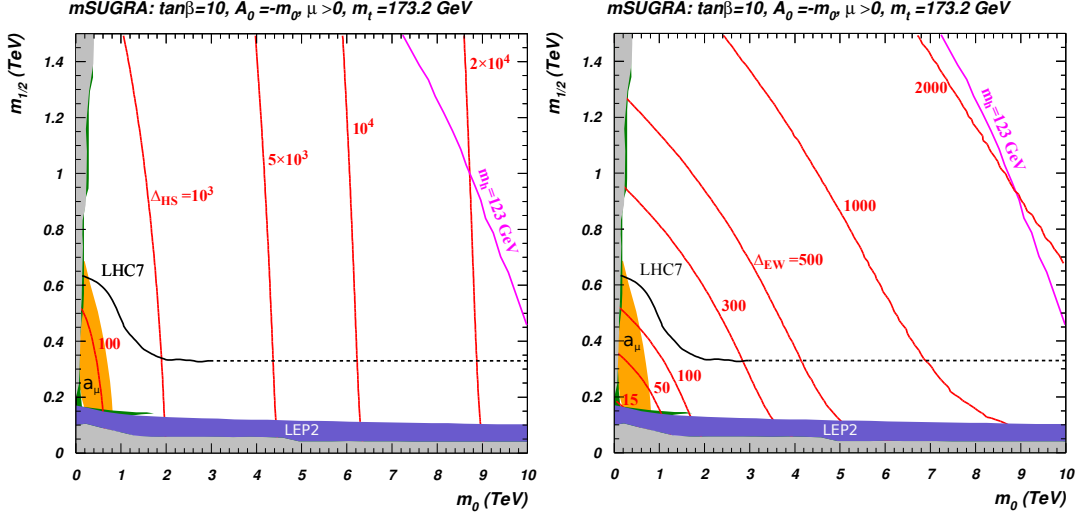


Figure 4: Contours of a) Δ_{HS} and b) Δ_{EW} in the mSUGRA model with $A_0 = -m_0$, $\tan \beta = 10$ and $\mu > 0$. The value of m_t as well as the various shaded/coloured regions are as in Fig. 2.

In Fig. 5, we show the m_0 vs. $m_{1/2}$ plane for $A_0 = -m_0$ but with $\tan \beta = 50$. We see this is qualitatively very similar to the previous figure aside from the sizeable LHCb excluded region on the low m_0 portion of the plane. Again the theoretically excluded region occurs at values of m_0 far beyond the range shown. Note though that the contour of $m_h = 123$ GeV has moved to slightly lower m_0 values. Still, requiring $m_h > 123$ GeV requires $\Delta_{\text{HS}} > 5 \times 10^3$, and $\Delta_{\text{EW}} \gtrsim 700$.

According to Ref. [6], large mixing in the top squark sector and consequently the largest values of m_h occur in mSUGRA for $A_0 \sim -2m_0$. In Fig. 6, we show contours of Δ_{HS} and Δ_{EW} for $\tan \beta = 10$ and $A_0 = -2m_0$. We note again that the HB/FP region does not appear in this plane. Notice also that the contours of $m_h = 123$ GeV have moved all the way down to $m_0 \sim 2$ TeV: thus, now much of the mSUGRA plane shown is *allowed* by the LHC Higgs-like resonance discovery. In fact, the portion of the plane with $m_0 \gtrsim 6 - 8$ TeV gives too large a value of $m_h > 127$ GeV. The portion of the m_0 vs. $m_{1/2}$ plane allowed by both LHC7 sparticle searches and by having $m_h \sim 123 - 127$ GeV requires $\Delta_{\text{HS}} \sim 10^3 - 10^4$, or 0.1-0.01% HSFT. The EWFT required is $\Delta_{\text{EW}} \gtrsim 10^3$, also large. The lesson learned here is that the remaining mSUGRA regions with $m_h \sim 123 - 127$ GeV, and which obey sparticle mass constraints, are highly fine-tuned, even with the less restrictive EWFT measure.

Fig. 7 shows the mSUGRA plane for $A_0 = -2m_0$ but with $\tan \beta = 50$. In this case, large theoretically excluded parameter regions appear and these only grow larger until the

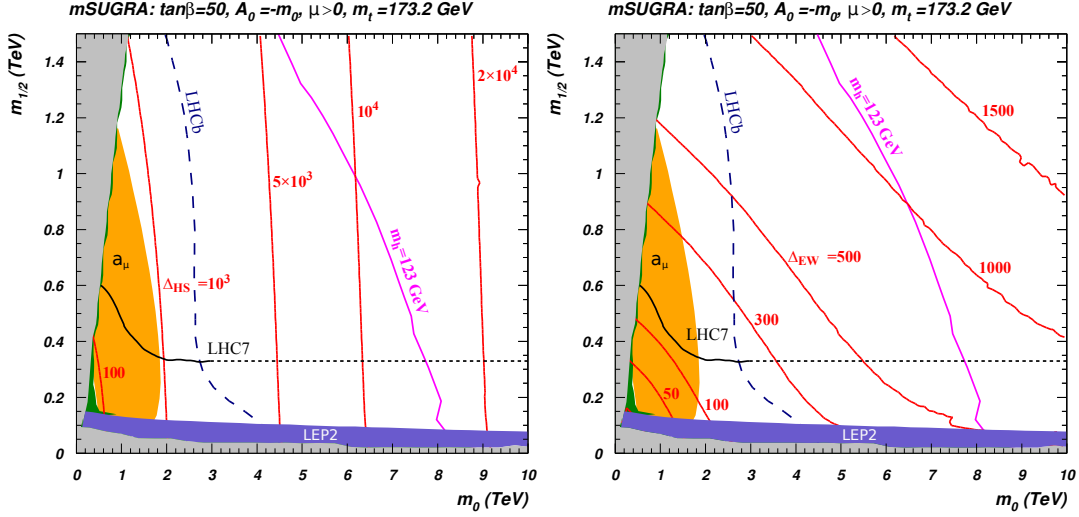


Figure 5: Contours of a) Δ_{HS} and b) Δ_{EW} in the mSUGRA model with $A_0 = -m_0$, $\tan \beta = 50$ and $\mu > 0$. The value of m_t as well as the various shaded/coloured regions are as in Fig. 3.

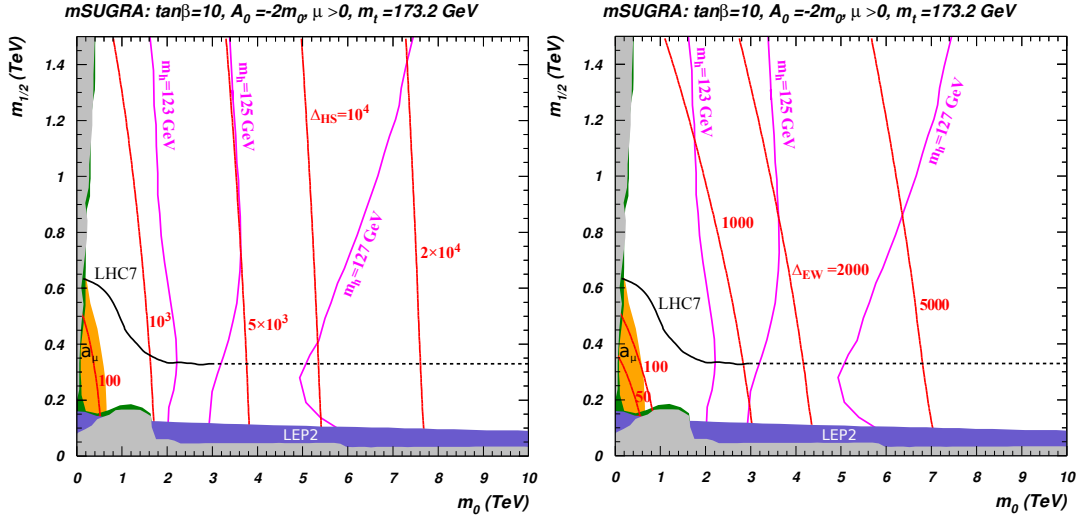


Figure 6: Contours of a) Δ_{HS} and b) Δ_{EW} in the mSUGRA model with $A_0 = -2m_0$, $\tan \beta = 10$ and $\mu > 0$. The value of m_t as well as the various shaded/coloured regions are as in Fig. 2.

entire parameter space collapses for even higher $\tan \beta \sim 55 - 60$ [33]. The region on the right is forbidden because m_A^2 turns negative, not because $|\mu|$ becomes small: this is why there is no DM-allowed region for large values of m_0 . The low $m_{1/2}$ and low m_0 portions of the plane marked LHCb are excluded due to too large a $B_s \rightarrow \mu^+ \mu^-$ branching fraction. The $m_h = 123$ GeV contour nearly coincides with $\Delta_{\text{HS}} = 10^3$ and $\Delta_{\text{EW}} = 500$. In this case, values of $m_0 \gtrsim 6$ TeV are excluded as giving rise to too heavy a value of m_h . Thus, again the regions with $m_h \sim 123 - 127$ GeV and obeying LHC7 sparticle search constraints, are highly fine-tuned.

Before closing this section, we digress to compare our results for the EWFT measure with some results in the recent literature [15] for the fine-tuning within the mSUGRA/CMSSM

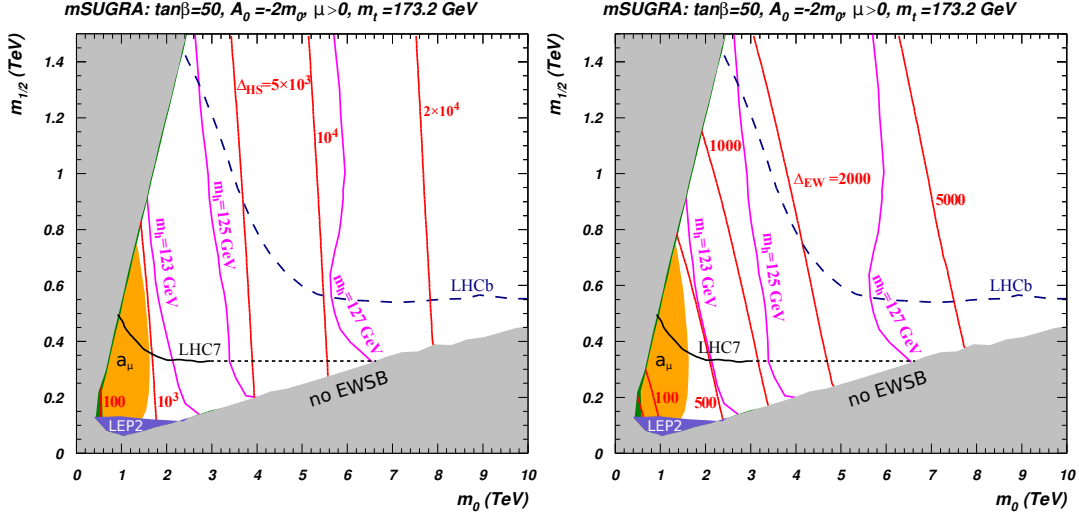


Figure 7: Contours of a) Δ_{HS} and b) Δ_{EW} in the mSUGRA model with $A_0 = -2m_0$, $\tan\beta = 50$ and $\mu > 0$. The value of m_t as well as the various shaded/coloured regions are as in Fig. 3.

model calculated using the procedure described at the end of Sec. 2.2. We have already argued at the end of that section that the fine-tuning measure that results from substituting $m_{H_u}^2$ in Eq. (2.7) and the analogous expression for $m_{H_d}^2$ into Eq. (2.3) should match our EWFT measure. To check this, we have compared our results in Fig. 2b) to those in Fig. 1 of the first paper of Ref. [15]. There, these authors show the *minimum* value of their fine-tuning parameter Δ in the $m_0 - m_{1/2}$ plane, marginalizing over a range of A_0 and $\tan\beta$. We see that the shapes of their Δ contours are qualitatively similar (except in the large m_0 region where the contours turn around because radiative correction effects are important) to those of the contours in frame b) of Figs. 2 and 3. We use our $A_0 = 0$ figures for this comparison because of all the figures these have the smallest value of Δ_{EW} . We have also checked that for any chosen value of m_0 and $m_{1/2}$ Δ of Antusch *et al.* has a magnitude similar to (but never larger than) the corresponding lowest Δ_{EW} that we obtain for any choice of A_0 and $\tan\beta$.

4. Scan over mSUGRA parameter space

While the results of the previous section provide an overview of both the EWFT and the HSFT measures in light of LHC7 and LHC8 constraints on sparticle and Higgs boson masses, we only presented results for particular choices of A_0 and $\tan\beta$, and for $\mu > 0$. In this Section, we present results from a scan over the complete mSUGRA parameter space with the following range of model parameters:

$$m_0 : 0 - 15 \text{ TeV}, \quad (4.1)$$

$$m_{1/2} : 0 - 2 \text{ TeV}, \quad (4.2)$$

$$-2.5 < A_0/m_0 < 2.5, \quad (4.3)$$

$$\tan\beta : 3 - 60. \quad (4.4)$$

We will show results for both $\mu > 0$ and $\mu < 0$. For each solution generated, we require

1. electroweak symmetry be radiatively broken (REWSB),
2. the neutralino \tilde{Z}_1 is the lightest MSSM particle,
3. the light chargino mass obeys the LEP2 limit that $m_{\tilde{W}_1} > 103.5$ GeV [24],
4. $m_h = 125 \pm 2$ GeV in accord with the recent Higgs-like resonance discovery at LHC [1, 2],
5. the calculated value of $BF(B_s \rightarrow \mu^+ \mu^-)$ lie within $(2 - 4.7) \times 10^{-9}$ in accord with recent LHCb measurements [26] and
6. the mass spectra obey LHC7 sparticle mass constraints for the mSUGRA model [8, 9].

Our first results are shown in Fig. 8 for *a*) Δ_{HS} and *b*) Δ_{EW} versus m_0 . Solutions with $\mu < 0$ are shown as blue circles while solutions with $\mu > 0$ are shown in red crosses. Note that here, and in subsequent figures, there are many points for $\mu < 0$ (red circles) that are not visible as these are covered by the red crosses for $\mu > 0$. In frame *a*), we see that Δ_{HS} values occupy a rather narrow band which increases monotonically with m_0 . Values of $m_0 \lesssim 1$ TeV are excluded by the requirement $m_h > 123$ GeV. The $\mu > 0$ and $\mu < 0$ solutions occupy essentially the same band. This is not surprising because the large logarithms are essentially independent of the sign of μ . The minimum allowed value of Δ_{HS} is ~ 1000 , so that at least 0.1% fine-tuning is required of all remaining mSUGRA solutions. The minimum for Δ_{HS} occurs at $m_0 \sim 1500$ GeV. This minimal Δ_{HS} solution is shown as a benchmark point in Sec. 5. For m_0 as high as 15 TeV, Δ_{HS} increases to nearly 10^5 . In frame *b*), we show Δ_{EW} versus m_0 . Here, the shape of the allowed region is very different from the Δ_{HS} case in frame *a*). Low values of m_0 can give $m_h > 123$ GeV only if $|A_0/m_0|$ is sizeable and, as we have already seen, yield Δ_{EW} of at least several hundred. Smaller values of Δ_{EW} are obtained only in the HB/FP region where m_0 is large. In other words, in the “hole region” in frame *b*), we have $m_h < 123$ GeV. The point with the minimum value of $\Delta_{\text{EW}} \sim 100$ occurs at $m_0 \sim 7900$ GeV, and is shown as the electroweak benchmark point in the next section. Over the remaining mSUGRA parameter space, at best 1% EWFT is required.

In Fig. 9, we show the distributions of Δ_{HS} and Δ_{EW} versus $m_{1/2}$. The sharp edge on the left is a reflection of the lower limit on $m_{\tilde{g}}$ from LHC7 searches. In frame *a*) for Δ_{HS} , we see that the minimal Δ_{HS} is spread across a wide spectrum of $m_{1/2}$ values. This is consistent with the behavior of Δ_{HS} shown in Fig. 2*a*) where the HSFT contours are nearly vertical, indicating little dependence on $m_{1/2}$. In frame *b*), the minimal values of Δ_{EW} are also spread across the $m_{1/2}$ range. For both Δ_{HS} and Δ_{EW} , there may be a slight preference for lower $m_{1/2}$ values.

In Fig. 10 we show how Δ_{HS} and Δ_{EW} are distributed versus A_0/m_0 . In frame *a*), we see that minimal $\Delta_{\text{HS}} \sim 1000$ is obtained for $A_0/m_0 \sim -2$, which is also the vicinity of where m_h is maximal for given m_0 and $m_{1/2}$ values. There is also a minimum at

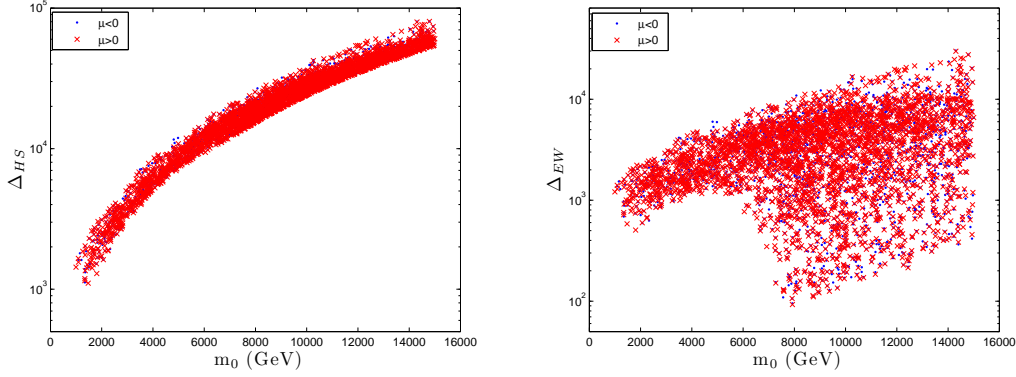


Figure 8: Fine-tuning measures Δ_{HS} and Δ_{EW} versus m_0 from a scan over mSUGRA/CMSSM parameter space for $\mu > 0$ (red crosses) and $\mu < 0$ (blue circles). We take $m_t = 173.2$ GeV.

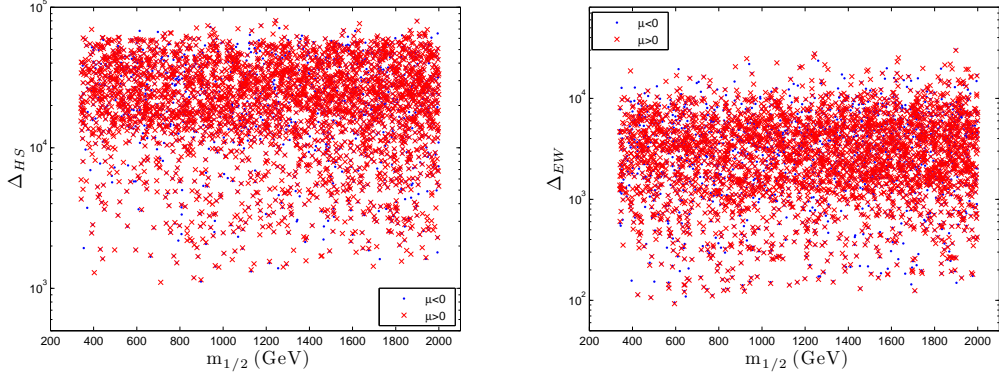


Figure 9: Fine-tuning measures Δ_{HS} and Δ_{EW} versus $m_{1/2}$ from a scan over mSUGRA/CMSSM parameter space for $\mu > 0$ (red crosses) and $\mu < 0$ (blue circles).

$A_0/m_0 \sim 2.5$, with Δ_{HS} reaching only to ~ 3000 ¹⁰. In frame b), the value of Δ_{EW} is even more correlated with A_0/m_0 . For $|A_0/m_0| \lesssim 1$, Δ_{EW} tends to be smaller than for larger values of $|A_0/m_0|$. The solutions with the least EWFT occur at $A_0/m_0 \sim \pm 0.6$, with the minimal $\Delta_{\text{EW}} \sim 100$. Once again, this occurs in the HB/FP region mentioned above. For larger magnitudes of A_0/m_0 , the HB/FP region is absent, and Δ_{EW} is much larger. The gap in the plots around $A_0/m_0 \sim 0$ occur because it is nearly impossible to generate m_h as heavy as 123 – 127 GeV for such low values of trilinear couplings[6].

In Fig. 11, we plot Δ_{HS} and Δ_{EW} versus $\tan \beta$. The minimal Δ_{HS} and Δ_{EW} solutions are spread uniformly across a range of $\tan \beta$ values. At very low $\tan \beta \lesssim 10$ values, it is difficult to generate solutions with $m_h \gtrsim 123$ GeV unless mSUGRA parameters are extremely large, leading to high fine-tuning.

¹⁰The asymmetry of the minimum of Δ_{HS} with respect to the sign of A_0 may only be a reflection of the fact that it is more difficult to generate large values of m_h for positive values of A_0 .

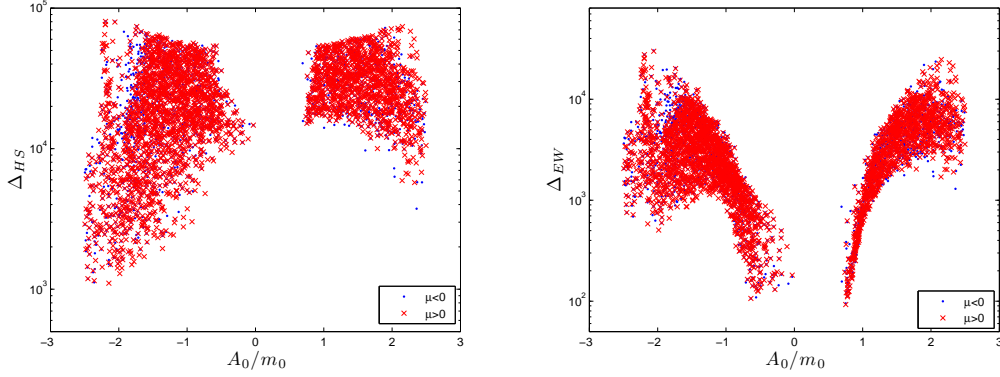


Figure 10: Fine-tuning measures Δ_{HS} and Δ_{EW} versus A_0/m_0 from a scan over mSUGRA/CMSSM parameter space for $\mu > 0$ (red crosses) and $\mu < 0$ (blue circles).

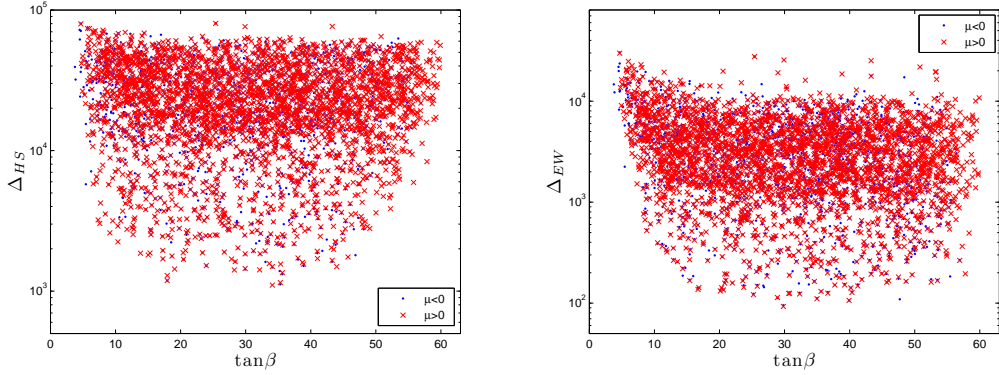


Figure 11: Fine-tuning measures Δ_{HS} and Δ_{EW} versus $\tan \beta$ from a scan over mSUGRA/CMSSM parameter space for $\mu > 0$ (blue circles) and $\mu < 0$ (red crosses).

5. Lowest fine-tuning mSUGRA benchmarks

What is apparent from our results so far is that, after imposing LHC7 sparticle mass constraints and requiring that $m_h = 125 \pm 2$ GeV on the mSUGRA/CMSSM model, the viable solutions are fine-tuned to at least 1% even with the less stringent EWFT measure. With a fine-tuning measure that knows about the high scale origin of mSUGRA parameters, the required fine-tuning is increased by an order of magnitude. Nonetheless, our understanding of how SUSY breaking parameters arise is extremely limited and it remains possible that nature may appear fine-tuned to a certain degree. With this in mind, we exhibit and qualitatively examine the features of the lowest Δ_{HS} and the lowest Δ_{EW} solutions in the mSUGRA/CMSSM framework. These are listed in Table 1 as solutions HS1 and EW1.

Solution HS1 has $\Delta_{HS} = 1100$ and so requires $\sim 0.1\%$ fine-tuning. The EWFT parameter $\Delta_{EW} \sim 600$, requiring $\sim 0.2\%$ fine-tuning. HS1 has $m_0 \sim 1500$ GeV, lying at the lower edge of the band of solutions shown in Fig. 8. With $m_{\tilde{g}} \sim 1660$ GeV, and $m_{\tilde{q}} \sim 2000$ GeV, this solution lies beyond the reach of LHC8 searches with up to 30 fb^{-1} [34], but should be accessible to LHC14 searches with $\sim 10 - 20 \text{ fb}^{-1}$ [35]. The relatively light top squarks

parameter	HS1	EW1
m_0	1472.0	7926.4
$m_{1/2}$	711.0	594.6
A_0	-3157.4	5968.2
$\tan \beta$	34.1	29.8
$m_{\tilde{g}}$	1662.5	1589.9
$m_{\tilde{u}_L}$	2058.8	7949.5
$m_{\tilde{u}_R}$	2025.4	7972.3
$m_{\tilde{e}_R}$	1494.7	7922.0
$m_{\tilde{t}_1}$	887.8	4547.6
$m_{\tilde{t}_2}$	1499.8	6197.4
$m_{\tilde{b}_1}$	1475.6	6175.2
$m_{\tilde{b}_2}$	1731.0	7406.6
$m_{\tilde{\tau}_1}$	1023.9	7187.3
$m_{\tilde{\tau}_2}$	1347.7	7563.8
$m_{\tilde{\nu}_\tau}$	1339.9	7565.6
$m_{\tilde{W}_2}$	1550.1	657.6
$m_{\tilde{W}_1}$	594.0	490.4
$m_{\tilde{Z}_4}$	1547.9	659.0
$m_{\tilde{Z}_3}$	1545.2	638.5
$m_{\tilde{Z}_2}$	591.9	487.7
$m_{\tilde{Z}_1}$	308.1	257.6
m_h	123.2	123.1
μ	1550.8	619.7
m_A	1626.8	6682.5
$\Omega_{\tilde{Z}_1}^{th} h^2$	12.3	9.4
$BF(b \rightarrow s\gamma) \times 10^4$	2.7	3.1
$BF(B_s \rightarrow \mu^+\mu^-) \times 10^9$	4.4	3.8
$\sigma^{SI}(\tilde{Z}_1 p)$ (pb)	1.4×10^{-11}	1.6×10^{-10}
Δ_{HS}	1105	1.5×10^4
Δ_{EW}	582.9	92.4

Table 1: Input parameters and masses in GeV units for the two mSUGRA/CMSSM benchmark points with the lowest values of Δ_{HS} and Δ_{EW} after imposing $m_h = 125 \pm 2$ GeV and also the LHC7 sparticle mass bounds. We take $m_t = 173.2$ GeV.

allow for $\tilde{g} \rightarrow t\tilde{t}_1$ decay at $\sim 100\%$, followed by $\tilde{t}_1 \rightarrow t\tilde{Z}_1$. Thus, gluino pair production will give rise to $t\tilde{t}\tilde{t} + E_T^{\text{miss}}$ events at LHC and may be searchable even in the multi-jet plus E_T^{miss} channel[36]. First generation squark pair production and corresponding $\tilde{q}\tilde{q}$ production will augment this rate since typically $\tilde{q} \rightarrow q\tilde{g}$ for first and second generation squarks. Production of second and third generation squarks will be suppressed by parton distribution functions. The HS1 solution has $\Omega_{\tilde{Z}_1}^{th} h^2 \sim 12$, so would produce too many neutralinos in the early universe under the standard cosmology. Late time entropy production[38] or

neutralino decay to a lighter state, *e.g.* $\gamma + axino$ in extended models[39], can bring such a model into accord with the measured relic abundance. The $b \rightarrow s\gamma$ branching fraction is somewhat below measured values, although additional flavor-violating Lagrangian soft terms could bring this value into accord with measurements without affecting LHC phenomenology.

The solution EW1 has $\Delta_{\text{HS}} \sim 1.5 \times 10^4$, but $\Delta_{\text{EW}} \sim 100$ so that the latter requires EWFT at the 1% level. The reader may wonder whether it makes sense to talk about low values of Δ_{EW} when Δ_{HS} is so much larger. In this connection, it may be worth allowing for the possibility that the mSUGRA framework may itself one day be derived from an underlying theory along with specific relations between seemingly unrelated mSUGRA parameters that lead to cancellations of the terms containing the large logarithms, as discussed at the end of Sec. 2.2. Returning to the EW1 point in the Table with $m_{\tilde{g}} \sim 1600$ GeV and $m_{\tilde{q}} \sim 6-8$ TeV, we see that this model is only accessible to LHC14 searches with $\sim 50 - 100 \text{ fb}^{-1}$ of integrated luminosity[35]. In this case, gluino pair production would be followed by gluino three-body decays to multi-jet plus multi-lepton plus E_T^{miss} final states. The final states would be rich in W and Z bosons, leading to distinctive signatures [37]. The thermally-produced neutralino abundance $\Omega_{\tilde{Z}_1}^{th} h^2 \sim 10$, so again a non-standard cosmology as well as an extension of the spectrum is needed to bring this solution in accord with the measured dark matter density.

Both HS1 and EW1 points will need yet other new physics to bring them in accord with the E821 measurement [30] of the muon magnetic moment if this discrepancy continues to hold up.

6. Concluding Remarks

The recent discovery of a 125 GeV Higgs-like resonance at LHC has set a strong new constraint on supersymmetric models. In addition, the lack of evidence for a SUSY signal at LHC now requires masses of strongly interacting sparticles in models such as mSUGRA/CMSSM to be above the 1 TeV scale. If LHC searches for sparticles continue without a new physics signal, then the little hierarchy problem – how to reconcile the Z and Higgs boson mass scale with the scale of SUSY breaking – will become increasingly acute in models such as mSUGRA.¹¹

In this paper, we have reported on results from the calculation of two measures of fine-tuning in the mSUGRA/CMSSM model. The first – Δ_{HS} which includes information about the high scale origin of mSUGRA parameters – is the more stringent one. The second, Δ_{EW} , depends only on the physical spectrum and couplings, and so is universal to all models that yield the same weak scale Lagrangian. Our results incorporate the latest constraints from LHC7 sparticle searches along with a light Higgs scalar with $m_h \sim 123 - 127$ GeV. We find $\Delta_{\text{HS}} \gtrsim 10^3$, or at best 0.1% fine-tuning. The more model-independent EWFT gives a

¹¹We do note that the little hierarchy problem may be solved within the context of the MSSM if we go to non-universal SUGRA models: see *e.g.* Ref. [14, 40]. Alternatively, invoking extra singlets[41] or extra vector-like matter[42] may provide additional contributions to m_h while maintaining light top squarks which seem to be required for low electroweak fine-tuning.

$\Delta_{EW} \gtrsim 10^2$, or at best 1% fine-tuning. The minimum value of Δ_{EW} tends to occur near the FP region which extends to large values of m_0 and $m_{1/2}$ but which does not always overlap with the neutralino relic density allowed HB region. We will leave it to the reader to assess how much fine-tuning is too much, and also how much credence one should give to Δ_{HS} in light of our ignorance of physics at or around the GUT scale¹².

From a scan over the entire mSUGRA/CMSSM parameter space including LHC sparticle and Higgs mass constraints, we do find viable regions where EWFT is at the 1% level, even for gluino and squark masses well beyond LHC reach. These regions are characterized by $m_0 \sim 8$ TeV and $A_0 \sim \pm 0.6m_0$. Since these points are spread across a wide range of $m_{1/2}$ values ranging up to and perhaps beyond 2 TeV, it appears that regions of parameter space with EWFT at the 0.5-1% levels (but with very large values of Δ_{HS}) will persist even after the most ambitious LHC SUSY searches are completed.

To conclude, we remind the reader it was the realization that SUSY can solve the *big hierarchy* problem which provided the rationale for low scale SUSY. This remains unaltered by LHC and Higgs mass constraints. The underlying hope was that with sparticles close to the weak scale, there would be no hierarchy problem. The data seem to indicate that, at least in the mSUGRA framework, EWFT at the percent level is mandatory. It is difficult to say whether these considerations point to the failure of the mSUGRA model, or whether the little hierarchy is the result of an incomplete understanding of how soft supersymmetry breaking parameters arise. While we continue to regard models with low EWFT as especially interesting, it appears difficult to unilaterally discard SUSY models that are fine-tuned at a fraction of a percent or a part per mille, given that these provide the solution of the much more pressing *big hierarchy problem*. Our results provide a quantitative measure for ascertaining whether or not the remaining mSUGRA/CMSSM model parameter space is excessively fine-tuned, and so could provide impetus for considering alternative SUSY models.

Acknowledgments

We thank R. Nevzorov for many discussions about fine-tuning, including discussions about the potential contributions from first and second generation of sfermions. We are also grateful to I. Gogoladze for raising the issue of the large logs at PHENO 2012, and to C. Csaki for clarifying conversations at this meeting. This work was supported in part by grants from the U. S. Department of Energy.

References

- [1] G. Aad *et al.* [ATLAS Collaboration], *Phys. Lett. B* **716** (2012) 1 [arXiv:1207.7214 [hep-ex]].
- [2] S. Chatrchyan *et al.* [CMS Collaboration], *Phys. Lett. B* **716** (2012) 30 [arXiv:1207.7235 [hep-ex]].

¹²Of course, if we take the mSUGRA model to be the final high scale theory, we would no doubt take Δ_{HS} to be our fine-tuning measure, but the judgement to be made is whether one should treat mSUGRA in this manner.

- [3] M. S. Carena and H. E. Haber, *Prog. Part. Nucl. Phys.* **50** (2003) 63 [[hep-ph/0208209](#)].
- [4] A. Chamseddine, R. Arnowitt and P. Nath, *Phys. Rev. Lett.* **49** (1982) 970; R. Barbieri, S. Ferrara and C. Savoy, *Phys. Lett.* **B 119** (1982) 343; N. Ohta, *Prog. Theor. Phys.* **70** (1983) 542; L. Hall, J. Lykken and S. Weinberg, *Phys. Rev.* **D 27** (1983) 2359.
- [5] G. Kane, C. Kolda, L. Roszkowski and J. Wells, *Phys. Rev.* **D 49** (1994) 6173.
- [6] H. Baer, V. Barger and A. Mustafayev, *Phys. Rev.* **D 85** (2012) 075010 [[arXiv:1112.3017](#) [[hep-ph](#)]]; for earlier work, see H. Baer, V. Barger, P. Huang and A. Mustafayev, *Phys. Rev.* **D 84** (2011) 091701 [[arXiv:1109.3197](#) [[hep-ph](#)]].
- [7] A. Arbey, M. Battaglia, A. Djouadi, F. Mahmoudi and J. Quevillon, *Phys. Lett.* **B 708** (2012) 162; M. Carena, S. Gori, N. R. Shah and C. E. M. Wagner, *J. High Energy Phys.* **1203** (2012) 014 [[arXiv:1112.3336](#) [[hep-ph](#)]]; S. Akula, B. Altunkaynak, D. Feldman, P. Nath and G. Peim, *Phys. Rev.* **D 85** (2012) 075001 [[arXiv:1112.3645](#) [[hep-ph](#)]]; M. Kadastik, K. Kannike, A. Racioppi and M. Raidal, *J. High Energy Phys.* **1205** (2012) 061 [[arXiv:1112.3647](#) [[hep-ph](#)]]; O. Buchmueller, R. Cavanaugh, A. De Roeck, M. J. Dolan, J. R. Ellis, H. Flacher, S. Heinemeyer and G. Isidori *et al.*, *Eur. Phys. J.* **C 72** (2012) 2020 [[arXiv:1112.3564](#) [[hep-ph](#)]]; J. Cao, Z. Heng, D. Li and J. M. Yang, *Phys. Lett.* **B 710** (2012) 665 [[arXiv:1112.4391](#) [[hep-ph](#)]]; U. Ellwanger, *J. High Energy Phys.* **1203** (2012) 044 [[arXiv:1112.3548](#) [[hep-ph](#)]]; W. D. Schlatter and P. M. Zerwas, *Eur. Phys. J.* **H 36** (2012) 579 [[arXiv:1112.5127](#) [[physics.hist-ph](#)]]; J. F. Gunion, Y. Jiang and S. Kraml, *Phys. Lett.* **B 710** (2012) 454 [[arXiv:1201.0982](#) [[hep-ph](#)]]; P. Fileviez Perez, *Phys. Lett.* **B 711** (2012) 353 [[arXiv:1201.1501](#) [[hep-ph](#)]]; A. B. Lahanas and V. C. Spanos, *J. High Energy Phys.* **1206** (2012) 089 [[arXiv:1201.2601](#) [[hep-ph](#)]]; T. G. Rizzo, *Phys. Rev.* **D 85** (2012) 055010 [[arXiv:1201.2898](#) [[hep-ph](#)]]; H. Baer, I. Gogoladze, A. Mustafayev, S. Raza and Q. Shafi, *J. High Energy Phys.* **1203** (2012) 047 [[arXiv:1201.4412](#) [[hep-ph](#)]]; Z. Kang, J. Li and T. Li, [arXiv:1201.5305](#) [[hep-ph](#)]; C. F. Chang, K. Cheung, Y. C. Lin and T. C. Yuan, *J. High Energy Phys.* **1206** (2012) 128 [[arXiv:1202.0054](#) [[hep-ph](#)]]; L. Aparicio, D. G. Cerdeno and L. E. Ibanez, *J. High Energy Phys.* **1204** (2012) 126 [[arXiv:1202.0822](#) [[hep-ph](#)]]; L. Roszkowski, E. M. Sessolo and Y. L. Tsai, [arXiv:1202.1503](#) [[hep-ph](#)]; K. A. Olive, *J. Phys. Conf. Ser.* **384** (2012) 012010 [[arXiv:1202.2324](#) [[hep-ph](#)]]; J. -J. Cao, Z. -X. Heng, J. M. Yang, Y. -M. Zhang and J. -Y. Zhu, *J. High Energy Phys.* **1203** (2012) 086 [[arXiv:1202.5821](#) [[hep-ph](#)]]; H. Baer, V. Barger and A. Mustafayev, *J. High Energy Phys.* **1205** (2012) 091; M. Hirsch, F. R. Joaquim and A. Vicente, [arXiv:1207.6635](#) [[hep-ph](#)].
- [8] G. Aad *et al.* (ATLAS collaboration), *Phys. Lett.* **B 710** (2012) 67 [[arXiv:1109.6572](#) [[hep-ex](#)]].
- [9] S. Chatrchyan *et al.* (CMS collaboration), *Phys. Rev. Lett.* **107** (2011) 221804.
- [10] A. Fowlie *et al.* [arXiv:1206.0264](#) [[hep-ph](#)]; O. Buchmueller *et al.* [arXiv:1207.7315](#) [[hep-ph](#)]; J. Cao, Z. Heng, J. Yang and J. Zhu [arXiv:1207.3698](#) [[hep-ph](#)].
- [11] R. Barbieri and G. Giudice, *Nucl. Phys.* **B 306** (1988) 63.
- [12] A similar measure of fine-tuning was used by R. Kitano and Y. Nomura, *Phys. Lett.* **B 631** (2005) 58 and *Phys. Rev.* **D 73** (2006) 095004.
- [13] A. Strumia, *J. High Energy Phys.* **1104** (2011) 073; S. Cassel, D. Ghilencea, S. Kraml, A. Lessa and G. Ross, *J. High Energy Phys.* **1105** (2011) 120; U. Ellwanger, G. Espitalier-Noel and C. Hugonie, *J. High Energy Phys.* **1109** (2011) 105; S. F. King, M. Muhlleitner and R. Nevzorov, *Nucl. Phys.* **B 860** (2012) 207 [[arXiv:1201.2671](#) [[hep-ph](#)]];

- M. Papucci, J. T. Ruderman and A. Weiler, *J. High Energy Phys.* **1209** (2012) 035 [arXiv:1110.6926 [hep-ph]]; C. Brust, A. Katz, S. Lawrence and R. Sundrum, *J. High Energy Phys.* **1203** (2012) 103; R. Essig, E. Izaguirre, J. Kaplan and J. G. Wacker, *J. High Energy Phys.* **1201** (2012) 074 [arXiv:1110.6443 [hep-ph]]; H. Baer, V. Barger, P. Huang and X. Tata, *J. High Energy Phys.* **1205** (2012) 109 [arXiv:1203.5539 [hep-ph]]; G. Ross and K. Schmidt-Hoberg, *J. High Energy Phys.* **1208** (2012) 074; M. Cahill-Rowley, J. Hewett, A. Ismail and T. Rizzo, arXiv:1206.5800; H. Baer, S. Kraml and S. Kulkarni, arXiv:1208.3039.
- [14] H. Baer, V. Barger, P. Huang, A. Mustafayev and X. Tata, *Phys. Rev. Lett.* **109** (2012) 161802 [arXiv:1207.3343 [hep-ph]].
- [15] S. Antusch, L. Calibbi, V. Maurer, M. Monaco and M. Spinrath, *Phys. Rev. D* **85** (2012) 035025 [arXiv:1111.6547 [hep-ph]]; S. Antusch, L. Calibbi, V. Maurer, M. Monaco and M. Spinrath, arXiv:1207.7236 [hep-ph].
- [16] H. Baer, F. E. Paige, S. D. Protopopescu and X. Tata, hep-ph/9305342; A. Djouadi, J. -L. Kneur and G. Moultaka, *Comput. Phys. Commun.* **176** (2007) 426; J. Conley, S. Gainer, J. Hewett, M. Le and T. Rizzo, *Eur. Phys. J. C* **71** (2011) 1697; S. Sekmen, S. Kraml, J. Lykken, F. Moortgat, S. Padhi, L. Pape, M. Pierini and H. B. Prosper *et al.*, *J. High Energy Phys.* **1202** (2012) 075.
- [17] C. Amsler *et al.* [Particle Data Group Collaboration], *Phys. Lett. B* **667** (2008) 1.
- [18] A. Freitas and Y. -C. Huang, *JHEP* **1208** (2012) 050.
- [19] K. L. Chan, U. Chattopadhyay and P. Nath, *Phys. Rev. D* **58** (1998) 096004; J. Feng, K. Matchev and T. Moroi, *Phys. Rev. Lett.* **84** (2000) 2322 and *Phys. Rev. D* **61** (2000) 075005; see also H. Baer, C. H. Chen, F. Paige and X. Tata, *Phys. Rev. D* **52** (1995) 2746 and *Phys. Rev. D* **53** (1996) 6241; H. Baer, C. H. Chen, M. Drees, F. Paige and X. Tata, *Phys. Rev. D* **59** (1999) 055014; for a model-independent approach, see H. Baer, T. Krupovnickas, S. Profumo and P. Ullio, *J. High Energy Phys.* **0510** (2005) 020.
- [20] M. Dine and A. E. Nelson, *Phys. Rev. D* **48** (1993) 1277 [hep-ph/9303230]; M. Dine, A. E. Nelson and Y. Shirman, *Phys. Rev. D* **51** (1995) 1362 [hep-ph/9408384].
- [21] H. Baer and M. Brhlik, *Phys. Rev. D* **53** (1996) 597; V. Barger and C. Kao, *Phys. Rev. D* **57** (1998) 3131.
- [22] O. Lebedev, H. P. Nilles and M. Ratz, hep-ph/0511320.
- [23] H. Baer, C. H. Chen, R. Munroe, F. Paige and X. Tata, *Phys. Rev. D* **51** (1995) 1046; H. Baer, J. Ferrandis, S. Kraml and W. Porod, *Phys. Rev. D* **73** (2006) 015010; ISAJET, by H. Baer, F. Paige, S. Protopopescu and X. Tata, hep-ph/0312045.
- [24] Joint LEP 2 Supersymmetry Working Group, *Combined LEP Chargino Results up to 208 GeV*, http://lepsusy.web.cern.ch/lepsusy/www/inos_moriond01/charginos_pub.html.
- [25] J. K. Mizukoshi, X. Tata and Y. Wang, *Phys. Rev. D* **66** (2002) 115003; H. Baer, C. Balazs, A. Belyaev, J. K. Mizukoshi, X. Tata and Y. Wang, *J. High Energy Phys.* **0207** (2002) 050.
- [26] R. Aaij *et al.* [LHCb Collaboration], arXiv:1211.2674.
- [27] IsaReD, see H. Baer, C. Balazs and A. Belyaev, *J. High Energy Phys.* **0203** (2002) 042.
- [28] WMAP Collaboration, E. Komatsu *et al.* *Astrophys. J. Suppl.* **192**, (2011) 18.

- [29] J. Ellis, T. Falk and K. Olive, *Phys. Lett. B* **444** (1998) 367; J. Ellis, T. Falk, K. Olive and M. Srednicki, *Astropart. Phys.* **13** (2000) 181; M.E. Gómez, G. Lazarides and C. Pallis, *Phys. Rev. D* **61** (2000) 123512 and *Phys. Lett. B* **487** (2000) 313; A. Lahanas, D. V. Nanopoulos and V. Spanos, *Phys. Rev. D* **62** (2000) 023515; R. Arnowitt, B. Dutta and Y. Santoso, *Nucl. Phys. B* **606** (2001) 59; see also Ref. [27].
- [30] Muon $g - 2$ Collaboration, G. Bennett *et al.* *Phys. Rev. D* **73** (2006) 072003.
- [31] M. Davier, A. Hoecker, B. Malaescu and Z. Zhang, *Eur. Phys. J. C* **71** (2011) 1515 [Erratum-ibid. C **72**, 1874 (2012)] [[arXiv:1010.4180](#) [hep-ph]].
- [32] J. Ellis and K. A. Olive, *Eur. Phys. J. C* **72** (2012) 2005.
- [33] H. Baer and C. Balazs, *JCAP* **0305** (2003) 006.
- [34] H. Baer, V. Barger, A. Lessa and X. Tata, *Phys. Rev. D* **85** (2012) 051701 [[arXiv:1112.3044](#) [hep-ph]].
- [35] H. Baer, X. Tata and J. Woodside, *Phys. Rev. D* **45** (1992) 142; H. Baer, C. H. Chen, F. Paige and X. Tata, *Phys. Rev. D* **52** (1995) 2746 and *Phys. Rev. D* **53** (1996) 6241; H. Baer, C. H. Chen, M. Drees, F. Paige and X. Tata, *Phys. Rev. D* **59** (1999) 055014; H. Baer, C. Balázs, A. Belyaev, T. Krupovnickas and X. Tata, *J. High Energy Phys.* **0306** (2003) 054; see also, S. Abdullin and F. Charles, *Nucl. Phys. B* **547** (1999) 60; S. Abdullin *et al.* (CMS Collaboration), *J. Phys. G* **28** (2002) 469 [[hep-ph/9806366](#)]; B. Allanach, J. Hetherington, A. Parker and B. Webber, *J. High Energy Phys.* **08** (2000) 017; H. Baer, V. Barger, A. Lessa and X. Tata, *J. High Energy Phys.* **0909** (2009) 063; H. Baer, V. Barger, A. Lessa and X. Tata, [arXiv:1207.4846](#) [hep-ph].
- [36] J. Bramante, J. Kumar and B. Thomas, *Phys. Rev. D* **86** (2012) 015014.
- [37] H. Baer, V. D. Barger, D. Karatas and X. Tata, *Phys. Rev. D* **36** (1987) 96; H. Baer, X. Tata and J. Woodside, *Phys. Rev. D* **42** (1990) 1450.
- [38] H. Baer, A. Lessa and W. Sreethawong, *JCAP* **1201** (2012) 036.
- [39] H. Baer, A. D. Box and H. Summy, *J. High Energy Phys.* **0908** (2009) 080.
- [40] H. Baer, V. Barger, P. Huang, D. Mickelson, A. Mustafayev and X. Tata, [arXiv:1212.2655](#) [hep-ph].
- [41] L. Hall, D. Pinner and J. T. Ruderman, *J. High Energy Phys.* **1204** (2012) 131; S. F. King, M. Muhlleitner and R. Nevzorov, *Nucl. Phys. B* **860** (2012) 207; J. F. Gunion, Y. Jiang and S. Kraml, *Phys. Lett. B* **710** (2012) 454; K. J. Bae, K. Choi, E. J. Chun, S. H. Im, C. B. Park and C. S. Shin, [arXiv:1208.2555](#) [hep-ph]. J. Cao, Z. Heng, J. M. Yang, Y. Zhang, J. Zhu, [arXiv:1202.5821](#) [hep-ph].
- [42] K. S. Babu, I. Gogoladze, P. Nath and R. M. Syed, *Phys. Rev. D* **85** (2012) 075002; S. P. Martin, *Phys. Rev. D* **81** (2010) 035004 and *Phys. Rev. D* **82** (2010) 055019; K. J. Bae, T. H. Jung and H. D. Kim, [arXiv:1208.3748](#) [hep-ph].